Metallic-nanoparticle assisted enhanced band-to-band tunneling current

Deblina Sarkar[a] and Kaustav Banerjee[a]
Department of Electrical and Computer Engineering, University of California, Santa Barbara, California 93106, USA

(Received 1 May 2011; accepted 27 July 2011; published online 30 September 2011)

Metallic nanoparticle assisted band-to-band tunneling is proposed, and the impact of such nanoparticle induced states on the tunneling probability and current is modeled and analyzed. An analytical formula for tunneling probability is derived for the case of constant force, and it is shown that the incorporation of these particles in the forbidden gap can lead to a substantial increase in the tunneling current. The effect of the Fermi-level pinning position on the tunneling current is studied, and the pinning value for obtaining maximum improvement in current is discussed depending on the force conditions. It is also shown that an asymmetric pinning is required to leverage maximum benefits from the insertion of metallic nanoparticles. © *2011 American Institute of Physics*. [doi:10.1063/1.3633343]

Tunnel-field-effect-transistor (TFET)[1–5] employing band-to-band tunneling (BTBT)[6–8] is a potential candidate for nanoscale device applications, due to its ability to overcome the 60 mV/decade fundamental limit of subthreshold swing in metal–oxide–semiconductor field-effect transistors (MOS-FETs). However, the TFETs face a major challenge because of their low ON-current. In this letter, we propose and show that the incorporation of metallic nanoparticles (MNs) at the tunnel-junction can lead to increased tunneling current. The current in TFETs is essentially limited by the barrier through which the tunneling occurs. For BTBT process, the tunneling barrier is determined by the bandgap of the semiconductor. A barrier is faced within the forbidden gap because of the absence of available states there to accommodate the electrons while the barrier reduces to zero at the conduction and valence band edges. If somehow states could be created within the forbidden gap of the semiconductor, it would lead to reduction in the effective tunneling barrier. This is precisely what can be achieved by the incorporation of metallic nanoparticles at the tunnel junction. When these nanoparticles are inserted, the barrier reduces to zero at the nanoparticles since metals have overlapping valence and conduction bands. Thus, essentially the tunnel-mechanism takes place in two steps: first step involves tunneling between the valence band of the semiconductor in segment-1 and the metal, while the second step involves that between the metal and the conduction band of the semiconductor in segment-2 as shown in Fig. 1(a). Growth of metallic islands within a semiconductor is possible, as has been demonstrated experimentally.[9–11]

To enable direct comparison of the metallic nanoparticle (MN) assisted tunneling probability with the well known Kane's formula,[7,12] we consider here the case of constant force (F) and similar effective masses for electrons and holes (m^*). Moreover, for such a case, an analytical formula for tunneling probability can be derived, which provides better physical insights. The insights developed here can be easily extended to non-uniform forces and non-symmetric effective masses.

For the standard case, i.e., without the presence of any states in the forbidden gap (E_G), the tunneling probability (T) according to Kane's formula gives $T = \exp(-\pi m^{*1/2} E_G^{3/2} / (2\sqrt{2} q\hbar F))$.

For tunneling between segment-1 and MN, we can write the tunneling probability from Fig. 1(b), using the Wentzel–Kramers–Brillouin (WKB) approximation and the two-band approximation[7] as

$$T = \exp\left(-2\int_0^{d_0} \sqrt{\frac{2m^*}{\hbar^2 E_G}\left(E_G qFx - (qFx)^2\right)}\,dx\right), \quad (1)$$

where E_G and m^* are the bandgap and carrier effective mass of the semiconductor material, respectively. It is to be noted that the tunneling probability here depends on the energy level at which tunneling occurs. This is because the region of integration determined by d_0, which we define as the tunneling length, is energy dependent and is given by (Fig. 1(b))

$$d_0 = (E_{\max} - E)/qF \quad \text{for} \quad (E_{\max} - E) < E_G \text{ and}$$
$$d_0 = E_G/qF \quad \text{for} \quad (E_{\max} - E) > E_G.$$

Finally from Eq. (1), an analytical formula for the tunneling probability is derived as

$$T = \exp\left(\begin{array}{l} \sqrt{\frac{m^*}{2E_G}}\frac{(qFE_G - 2q^2F^2d_0)\sqrt{qFE_Gd_0 - q^2F^2d_0^2}}{\hbar q^2F^2} \\ -\frac{1}{2\sqrt{2}}\frac{\sqrt{m^*}E_G^{3/2}}{q\hbar F}\tan^{-1}\left(\frac{qF(d_0 - E_G/2qF)}{\sqrt{qFE_Gd_0 - q^2F^2d_0^2}}\right) \\ -\frac{1}{8}\frac{\pi\sqrt{2}m^{*1/2}E_G^{3/2}}{q\hbar F} \end{array}\right). \quad (2)$$

In Fig. 2, the tunneling probability in Eq. (2) is plotted as a function of energy level E (as shown in Fig. 1(b)) for two different forces. It can be observed that for the MN-tunneling, the tunneling probability increases with E. This is due to the decrease in tunneling length d_0 with the increase in E. For the standard case, d_0 is given by E_G/qF (as shown in Fig. 1(c)), which is independent of E, and hence, the tunneling probability remains constant with E.

So far, we discussed the tunneling probability through one segment taken separately, which we will now use to calculate the current (that depends on the probabilities of both

[a]Authors to whom correspondence should be addressed. Electronic addresses: deblina@ece.ucsb.edu and kaustav@ece.ucsb.edu.

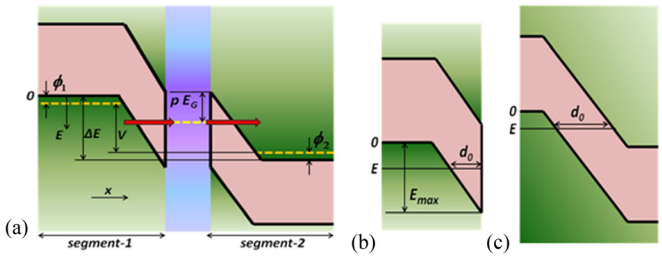

FIG. 1. (Color online) (a) Schematic band diagram of a tunnel junction where metallic nanoparticles have been incorporated leading to zero bandgap between segment-1 and segment-2. Due to the presence of the nanoparticles, tunneling process can now be divided into two parts: through segment-1 and segment-2 (denoted by horizontal arrows). V is the voltage applied across the junction. ϕ_1 (ϕ_2) denote the energy differences between the valence (conduction) band in segment-1 (segment-2) and the Fermi level. The Fermi level pinning position at the metal-semiconductor interface is denoted by p which is defined from the conduction band as a fraction of the bandgap (E_G). Segment-1 is shown separately in (b), highlighting the energy dependent (0 to E_{max}) tunneling length (d_0), while for (c) the standard case without any nanoparticles, d_0 is independent of energy (E). Note that the constant force (linear band bending) is assumed to derive analytical expressions. In real devices, Poisson-Schrodinger equations should be solved simultaneously for calculation of actual band-bending.

the segments taken together). On application of a voltage V across the junction, the applied voltage gets divided among the left and right segments (Fig. 1(a)). The fraction of the voltage dropped in each segment depends on the Fermi-level pinning position and the doping in the segments and can be calculated using the condition of continuity of current flowing through segment-1 and segment-2 where the equation of current though each segment can be written according to

$$I = \frac{2q}{h}\int_0^{\Delta E} T(E)\big(f_i(E) - f_f(E)\big)dE. \tag{3}$$

Here f_i and f_f denote the Fermi functions of the initial and final states from and to which the tunneling occurs, respectively. Here, ΔE denotes the energy window over which the current flows as shown in Fig. 1(a).

In Fig. 3, the current is plotted as a function of the Fermi level pinning position (p), which is defined from the conduction band edge as a fraction of the bandgap (Fig. 1(a)). It is observed that depending on the forces applied in the two segments, there is always an optimum value of p, which leads to the highest current. When the force in the two segments are equal, the peak current is obtained when the Fermi-level is

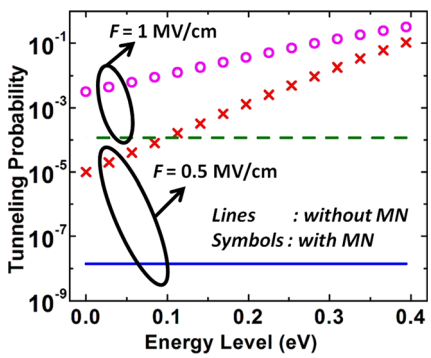

FIG. 2. (Color online) Tunneling probability as a function of energy level E (shown in Fig. 1(b)) highlighting the energy dependence of MN-tunneling probability. For all figures in this paper, $E_G = 0.93$ eV and $m^* = 0.064\, m_0$.

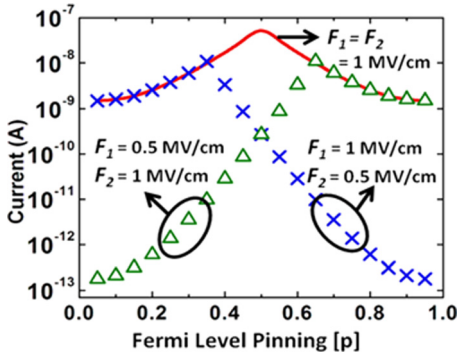

FIG. 3. (Color online) Current as a function of Fermi level pinning position p (defined in Fig. 1(a)) for similar ($F_1 = F_2$) as well as dissimilar ($F_1 \neq F_2$) forces in the two segments. For $F_1 = F_2$, the peak current occurs at $p = 0.5$, while for $F_1 \neq F_2$, the peak position shifts depending on the forces. The fraction of voltage drop and hence the depletion region width in each segment (in Fig. 1(a)) change so that the current continuity is satisfied.

pinned at the midgap ($p = 0.5$) while it decreases at either ends. This is because when $p = 0.5$, the band bending is symmetrical in both segments, voltage being equally divided ($= V/2$) between segment-1 and segment-2. Hence, the maximum value of tunneling length (in each segment) is given by (Fig. 1(a)),

$$d_{0\_\max\_mid} = \frac{E_{\max\_mid}}{qF} = \frac{E_G/2 + V/2 + \phi}{qF}. \tag{4}$$

Here, the subscript *mid* denotes that the Fermi level pinning occurs at the midgap ($E_G/2$) and we consider $\phi_1 = \phi_2 = \phi$. The symbol E_{max} is defined in Fig. 1. Now, when p is either smaller or greater than 0.5, then on one segment, the maximum value of tunneling length will be greater than $d_{0\_max\_mid}$, while on the other, it would be less than $d_{0\_max\_mid}$. Since the current is dominated by the most resistive region, the increased d_0 in one of the segments will lead to decrease in the current. When the forces in the two segments are considered to be different, then the current peak will occur away from $p = 0.5$ due to the asymmetry caused by the different forces.

Fig. 4 shows the current as a function of force, which is taken to be same in both the segments. Fermi-level pinning is considered to be at $p = 0.5$. It is clear that the current is increased significantly due to MN-tunneling compared to that without the incorporation of nanoparticles. Improvement in current of about 3 orders of magnitude at lower values of force and around 2 orders at higher forces is obtained.

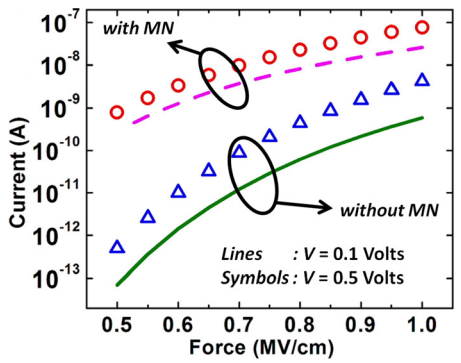

FIG. 4. (Color online) Current as a function of the force ($F_1 = F_2$) for two different values of V and $p = 0.5$. It is observed that MN-tunneling leads to a substantial increase in current compared to those without MN.

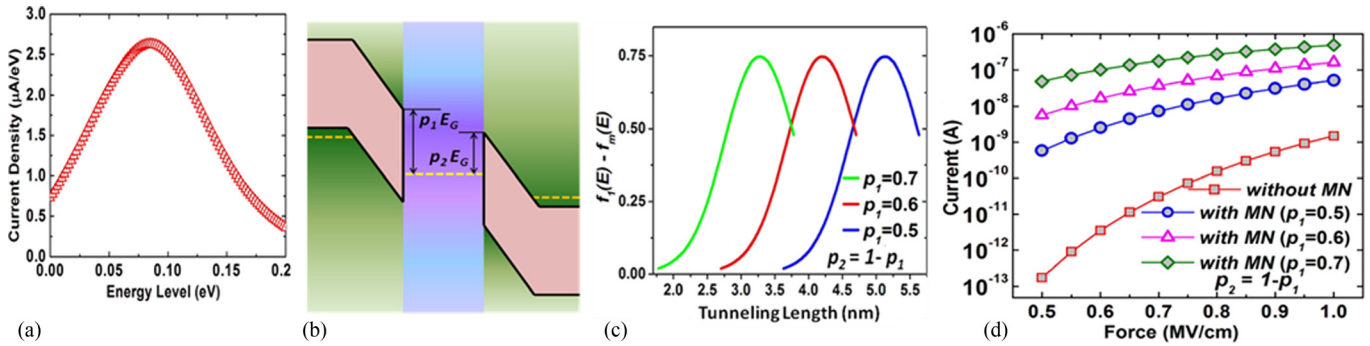

FIG. 5. (Color online) (a) Current density as a function of the energy level E plotted from 0 to ΔE. It is seen that the current initially increases with increase in E due to increase in the tunneling probability, but then decreases due to decrease in $(f_i(E) - f_f(E))$. (b) Schematic band diagram showing different pinning positions defined by p_1 and p_2 at the two segments where $p_1 > 0.5$ while $p_2 < 0.5$. (c) The difference in Fermi function between the left segment and the metal given by $(f_1(E) - f_m(E))$ as a function of the tunneling length for different p_1 with $p_2 = 1 - p_1$. We observe that as p_1 increases, the window of tunneling length over which current flows (which also corresponds to the energy window ΔE) shifts towards lower values of tunneling lengths. (d) Effective increase in the tunneling current with increase in p_1.

Till now we have considered the pinning level to be same for both the segments and found that $p = 0.5$ leads to the maximum current value for similar force in both regions. From Fig. 1(b) and Fig. 2, it is observed that maximum tunneling probability occurs at the highest value of E as it corresponds to the lowest value of d_0. However, on plotting the current density as a function of E (Fig. 5(a)), we observe that the current initially increases with increase in E. However, with further increase in E, the current decreases again. This is because with increase in E, the number of vacant states, into which the particle can tunnel to, reduces (or in other words $f_f(E)$ in Eq. (3) increases) and becomes particularly small as E goes down from the Fermi-level of the metal. Thus, though the $T(E)$ term in the expression for current in Eq. (3) increases with E, the current decreases due to the decrease in the term $(f_i(E) - f_f(E))$. Thus, we are not able to harness the full advantage of the very high tunneling probability at larger E. Now, let us explore whether further improvement can be achieved through use of dissimilar pinning levels in the two segments, which we will now refer to as p_1 and p_2. It is to be noted that the tuning of pinning level at the metallic nanoparticles has been demonstrated experimentally.[11] We observe that if we use dissimilar Fermi level pinning at the two segments such that at segment-1, pinning is more towards the valence band, i.e., $p_1 > 0.5$, while at segment-2, pinning is more towards the conduction band, i.e., $p_2 < 0.5$, as shown in Fig. 5(b), then we could effectively use the regions with higher E or smaller d_0 with higher tunneling probability. It is seen clearly from Fig. 5(c) that as the p_1 increases and p_2 decreases, the region over which the tunneling occurs shifts towards smaller values of d_0 in both segments. In Fig. 5(d), the current is plotted as a function of force for dissimilar p_1 and p_2 with p_2 set to $1 - p_1$. We observe that with increase in p_1, the current increases substantially and we get much higher current than what we achieved using identical pinning level for the two segments.

In this paper, for simplifying calculations, we have taken the occupation function at the nanoparticles to behave like a Fermi function within the window ΔE. In general, the occupation function at the nanoparticles can be expressed as a combination of the Fermi functions at segments 1 and 2, and it will behave like a Fermi function within ΔE for small biases. Also, in this paper, we have treated the MN-assisted tunneling in the *non-coherent* limit (since during the 2nd tunneling step, phase information of the 1st tunneling step is lost). Simulations capturing varying degree of coherence will require a full-fledged quantum-mechanical treatment involving severe computational complexity and is not discussed here. For design of MN-assisted tunnel-FETs, vertical transport leading to electron injection at energies above the valence band of the semiconductor at the source should be minimized in order to reduce the leakage currents. This can be ensured by making the size of the nanoparticles much smaller than the carrier inelastic scattering length.

In summary, metallic-nanoparticle assisted tunneling is proposed for improving the band-to-band tunneling current. An analytical formula for tunneling probability is derived and the Fermi-level pinning position leading to maximum improvement in current is determined. The case of dissimilar pinning at the two nanoparticle-semiconductor interfaces is also discussed. Thereby, it is shown that through judicious incorporation of metallic nanoparticles at the tunneling junction, the tunneling current can be improved significantly, which can be exploited in designing tunnel-FETs with higher ON currents.

This work was supported by the National Science Foundation, Grant No. CCF-0811880. Authors would like to thank A. C. Gossard and C. J. Palmstrøm at UCSB for their useful discussions.

[1]J. Appenzeller, Y. M. Lin, J. Knoch, and P. Avouris, Phys. Rev. Lett. **93**, 196805 (2004).
[2]K. K. Bhuwalka, S. Sedlmaier, A. K. Ludsteck, C. Tolksdorf, J. Schulze, and I. Eisele, IEEE Trans. Electron Devices **51**, 279 (2004).
[3]P. F. Wang, K. Hilsenbeck, T. Nirschl, M. Oswald, C. Stepper, M. Weis, D. Schmitt-Landsiedel, and W. Hansch, Solid State Electron. **48**, 2281 (2004).
[4]Q. Zhang, W. Zhao, and A. Seabaugh, IEEE Electron Device Lett. **27**, 297 (2006).
[5]W. Y. Choi, B.-G. Park, J. D. Lee, and T.-J. K. Liu, IEEE Electron Device Lett. **28**, 743 (2007).
[6]L. V. Keldysh, Sov. Phys. JETP **6**, 763 (1958).
[7]E. O. Kane, J. Phys. Chem. Solids **12**, 181 (1959).
[8]D. Sarkar, M. Krall, and K. Banerjee, Appl. Phys. Lett. **97**, 263109 (2010).
[9]D. C. Driscoll, M. P. Hansona, E. Mueller, and A. C. Gossard, J. Cryst. Growth **251**, 243 (2003).
[10]T. E. Buehl, J. M. LeBeau, S. Stemmer, M. A. Scarpulla, C. J. Palmstrøm, and A. C. Gossard, J. Cryst. Growth **312**, 2089 (2010).
[11]M. P. Hansona, D. C. Driscoll, E. Muller, and A. C. Gossard, Physica E **13**, 602 (2002).
[12]S. M. Sze, *Physics of Semiconductor Devices*, 3rd ed. (Wiley, New York, 2007).